Drug Metabolism and Disposition: DMD-AR-2021-000799

Target-Mediated Drug Disposition Affects the Pharmacokinetics of Interleukin-10 Fc-fusion Proteins at Pharmacologically Active Doses

Authors: Zheng Yang, Surendran Rajendran, Vanessa Spires, Brian Poirson, Murali Gururajan, Zheng Lin, Jaren Arbanas, Stanley Krystek, James Loy, Yuan Cheng, Stephen Carl, Samantha Pace, Yun Wang, John Mehl, Shihua Xu, Krishna Vasudevan, Miranda Broz, Lois Lehman-McKeeman, Paul Morin, and Robert F. Graziano

Affiliation: Bristol Myers Squibb Company, Princeton, New Jersey, U.S.A.

SUPPLEMENTAL MATERIALS AND REAGENTS

1. Structural Sequences of IL-10 and IL-10 Fc-fusion Proteins

mIL-10

```
1    SRGQY SREDN NCTHF PVGQS HMLLE LRTAF SQVKT FFQTK
41   DQLDN ILLTD SLMQD FKGYL GCQAL SEMIQ FYLVE VMPQA
81   EKHGP EIKEH LNSLG EKLKT LRMRL RRCHR FLPCE NKSKA
121  VEQVK SDFNK LQDQG VYKAM NEFDI FINCI EAYMM IKMKS
```

hIL-10

```
1    SRGQG TQSEN SCTHF PGNLP NMLRD LRDAF SRVKT FFQMK
41   DQLDN LLLKE SLLED FKGYL GCQAL SEMIQ FYLEE VMPQA
81   ENQDP DIKAH VNSLG ENLKT LRLRL RRCHR FLPCE NKSKA
121  VEQVK NAFNK LQEKG IYKAM SEFDI FINYI EAYMT MKIRN
```

mFc-mIL-10

```
1    VPRDCGCKPC ICTVPEVSSV FIFPPKPKDV LTITLTPKVT CVVVAISKDD
51   PEVQFSWFVD DVEVHTAQTQ PREEQFNSTF RSVSELPIMH QDWLNGKEFK
101  CRVNSAAFPA PIEKTISKTK GRPKAPQVYT IPPPKEQMAK DKVSLTCMIT
151  DFFPEDITVE WQWNGQPAEN YKNTQPIMDT DGSYFVYSKL NVQKSNWEAG
201  NTFTCSVLHE GLHNHHTEKS LSHSPGGGGG SGGGGSGGGG SGGGGSSRGQ
251  YSREDNNCTH FPVGQSHMLL ELRTAFSQVK TFFQTKDQLD NILLTDSLMQ
301  DFKGYLGCQA LSEMIQFYLV EVMPQAEKHG PEIKEHLNSL GEKLKTLRMR
351  LRRCHRFLPC ENKSKAVEQV KSDFNKLQDQ GVYKAMNEFD IFINCIEAYM
401  MIKMKS
```

hFc-hIL-10

```
1     DKTHTCPPCP APEAEGAPSV FLFPPKPKDT LMISRTPEVT CVVVDVSHED
51    PEVKFNWYVD GVEVHNAKTK PREEQYNSTY RVVSVLTVLH QDWLNGKEYK
101   CKVSNKALPA PIEKTISKAK GQPREPQVYT LPPSREEMTK NQVSLTCLVK
151   GFYPSDIAVE WESNGQPENN YKTTPPVLDS DGSFFLYSKL TVDKSRWQQG
201   NVFSCSVMHE ALHNHYTQKS LSLSPGGGGG SSGGGGSGGG GSGGGGSSPG
251   QGTQSENSCT HFPGNLPNML RDLRDAFSRV KTFFQMKDQL DNLLLKESLL
301   EDFKGYLGCQ ALSEMIQFYL EEVMPQAENQ DPDIKAHVNS LGENLKTLRL
351   RLRRCHRFLP CENKSKAVEQ VKNAFNKLQE KGIYKAMSEF DIFINYIEAY
401   MTMKIRN
```

hFc-hIL-10 mutant

```
1     DKTHTCPPCP APEAEGAPSV FLFPPKPKDT LMISRTPEVT CVVVDVSHED
51    PEVKFNWYVD GVEVHNAKTK PREEQYNSTY RVVSVLTVLH QDWLNGKEYK
101   CKVSNKALPA PIEKTISKAK GQPREPQVYT LPPSREEMTK NQVSLTCLVK
151   GFYPSDIAVE WESNGQPENN YKTTPPVLDS DGSFFLYSKL TVDKSRWQQG
201   NVFSCSVMHE ALHNHYTQKS LSLSPGGGGG SSGGGGSGGG GSGGGGSSPG
251   QGTQSENSCT HFPGNLPNML SDLRDAFSRV KTFFSMKDQL DNSLLKESLL
301   EDFKGYLGCQ ALSEMIQFYL EEVMPQAENQ DPDIKAHVNS LGENLKTLRL
351   RLRRCHRFLP CENKSKAVEQ VKNAFNKLQE KGIYKAMSEF DIFINYIEAY
401   MTMKIRN
```

2. Characterizations of IL-10 and IL-10 Fc-fusion Proteins

	mIL-10	hIL-10	mFc-mIL-10	hFc-hIL-10	hFc-hIL-10 Mutant
Molecular Weight (Da)*	18,751	18,703	91,004	90,815	90,542
Aggregation status					
High molecular weight aggregates	<5%	<5%	<5%	<5%	<5%
Low molecular weight components	<5%	<5%	<5%	<5%	<5%
Endotoxin (EU/mL)	<0.075	<0.075	<0.075	<0.075	<0.075

*Theoretical mass of deglycosylated form.

Primary structures of all five protein analytes (mIL-10, hIL-10, mFc-mIL-10, hFc-hIL10, and hFc-hIL-10 mutant) used in this publication were confirmed by LC/MS/MS peptide mapping with >97% sequence coverage. The molecular weights of the intact versions of these proteins verified by LC/MS were consistent with the theoretical masses calculated from the respective protein amino acid sequences.

SUPPLEMENTAL TABLE

Supplemental Table 1. Key Models Tested and Fitting Performance for mFc-mIL-10 Pharmacokinetic Data after Intravenous and Intraperitoneal Administration to Tumor- and Non-tumor-bearing Mice

Model	Objective function[a,b]	Akaike information criterion[b]	Schwarz-Bayesian information criterion[b]
1-compartment model with target- and non-target-mediated elimination	839	869	897
2-compartment model with target-mediated elimination only	839	870	900
2-compartment model with target- and non-target-mediated elimination (**final model**)	812	842	874

a. Expressed as -2 times the log-likelihood function.
b. Converted from the output statistics in SAAM II.

Supplemental Table 2. Key Models Tested and Fitting Performance for hFc-hIL-10 Pharmacokinetic Data after Intravenous Administration to Non-tumor-bearing Mice

Model	Objective function[a,b]	Akaike information criterion[b]	Schwarz-Bayesian information criterion[b]
1-compartment model with target- and non-target-mediated elimination	409	424	432
2-compartment model with target-mediated elimination only	407	422	432
2-compartment model with target- and non-target-mediated elimination (**final model**)	357	375	387

a. Expressed as -2 times the log-likelihood function.
b. Converted from the output statistics in SAAM II.

Supplemental Table 3. Key Models Tested and Fitting Performance for mIL-10 Pharmacokinetic Data after Intravenous Administration to Non-tumor-bearing Mice

Model	Objective function[a,b]	Akaike information criterion[b]	Schwarz-Bayesian information criterion[b]
1-compartment model with non-target-mediated elimination only	4,335	4,320	4,320
2-compartment model with target- and non-target-mediated elimination[c]	404	414	421
2-compartment model with non-target-mediated elimination only (**final model**)	407	418	421

a. Expressed as -2 times the log-likelihood function.
b. Converted from the output statistics in SAAM II.
c. The target binding affinity of mIL-10 was assumed to be the same as that (3.2 nM) of mFc-mIL-10 in mice.

Supplemental Table 4. Key Models Tested and Fitting Performance for hIL-10 Pharmacokinetic Data after Intravenous Administration to Non-tumor-bearing Mice

Model	Objective function[a,b]	Akaike information criterion[b]	Schwarz-Bayesian information criterion[b]
1-compartment model with non-target-mediated elimination only	2,490	2,492	2,492
2-compartment model with target- and non-target-mediated elimination[c]	261	273	277
2-compartment model with non-target-mediated elimination only (**final model**)	280	290	294

a. Expressed as -2 times the log-likelihood function.

b. Converted from the output statistics in SAAM II.

c. The target binding affinity of hIL-10 was assumed to be the same as that (2.9 nM) of hFc-hIL-10 in mice.

SUPPLEMENTAL FIGURE

Supplemental Figure 1. Diagnostic Plots Obtained from Pharmacokinetic Modeling of mFc-mIL-10 Average Concentration Data after Intravenous and Intraperitoneal Administration to Tumor- and Non-tumor-bearing Mice

a. Predicted vs. observed concentrations

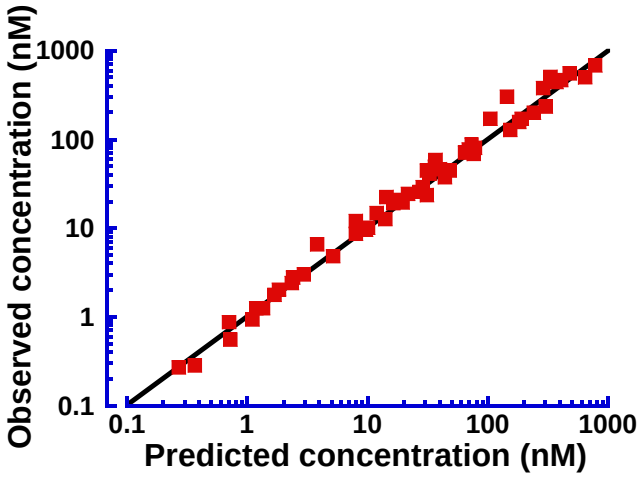

b. Weighted residuals vs. predicted concentrations

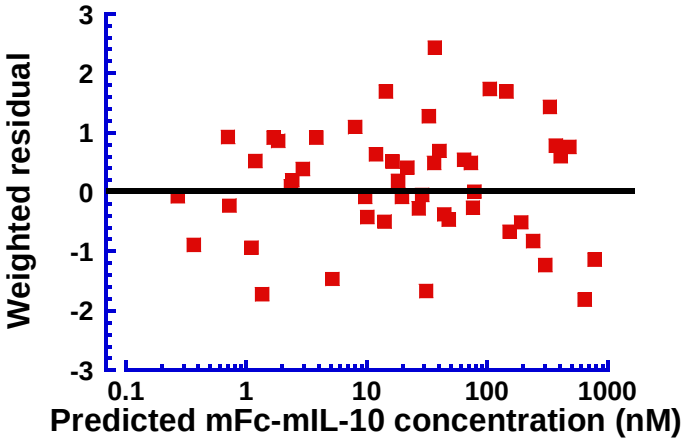

Supplemental Figure 2. Diagnostic Plots Obtained from Pharmacokinetic Modeling of hFc-hIL-10 Average Concentration Data after Intravenous Administration to Non-tumor-bearing Mice

a. Predicted vs. observed concentrations

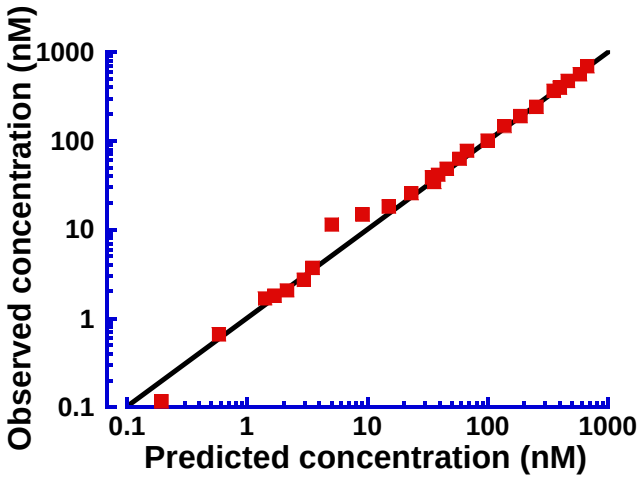

b. Weighted residuals vs. predicted concentrations

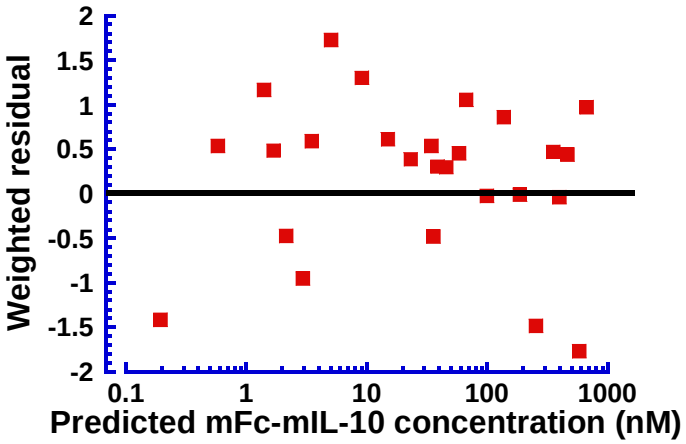

Supplemental Figure 3. Diagnostic Plots Obtained from Pharmacokinetic Modeling of mIL-10 Average Concentration Data after Intravenous Administration to Non-tumor-bearing Mice

a. Predicted vs. observed concentrations

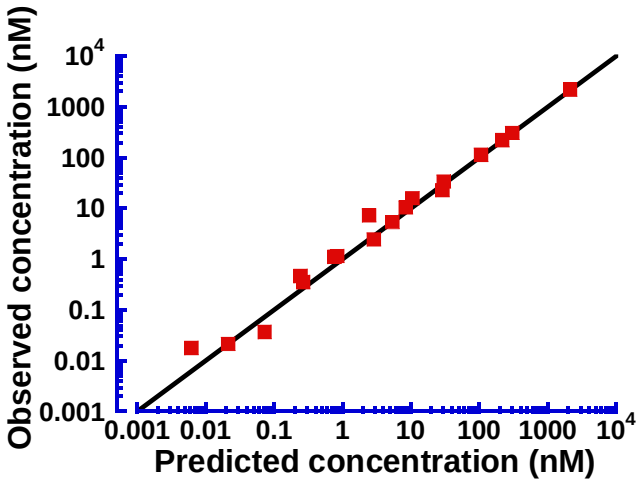

b. Weighted residuals vs. predicted concentrations

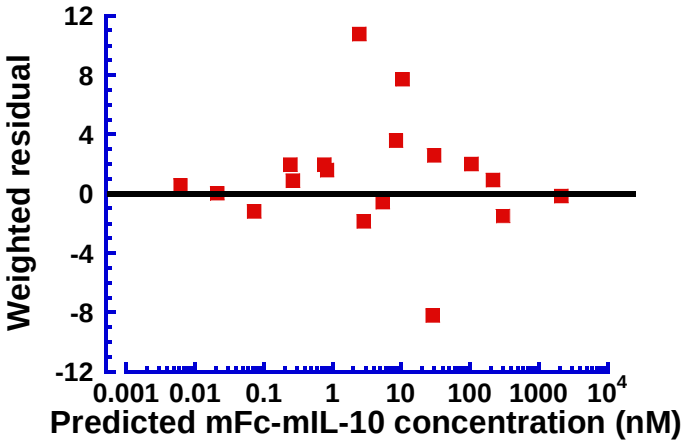

Supplemental Figure 4. Diagnostic Plots Obtained from Pharmacokinetic Modeling of hIL-10 Average Concentration Data after Intravenous Administration to Non-tumor-bearing Mice

a. Predicted vs. observed concentrations

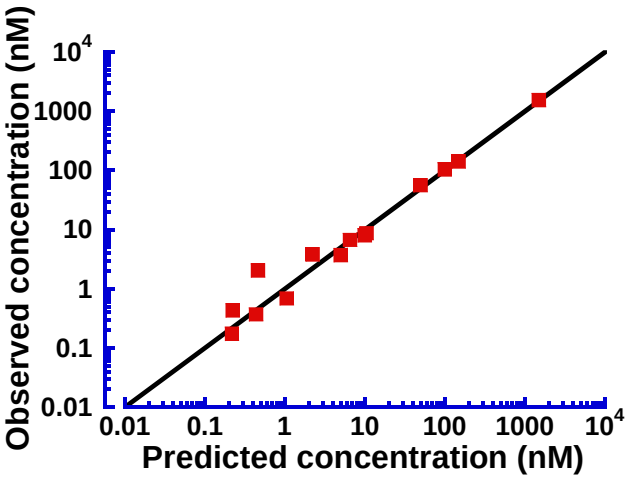

b. Weighted residuals vs. predicted concentrations

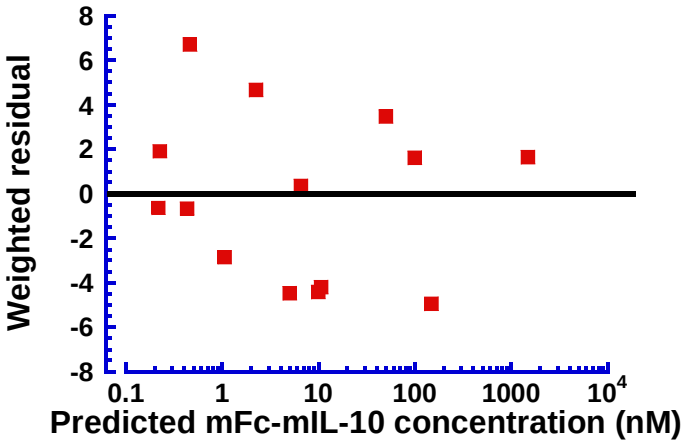

Supplemental Figure 5. **Time Course of Anti-mFc-mIL-10 Antibody Titers in the Mouse CT26 Syngeneic Tumor Model following Intraperitoneal Administration of mFc-mIL-10 and a Mouse Anti-mPD-1 Monoclonal Antibody**

(Note: mFc-mIL-10 was dosed weekly (QW) for 3 doses and the mouse anti-mPD-1 monoclonal antibody was given every 4 days (Q4D) for 6 doses. Anti-mFc-mIL-10 antibodies in mouse serum samples were detected by a ligand-binding assay on a chemiluminescence platform developed at Bristol Myers Squibb, with mFc-mIL-10 and peroxidase AffiniPure rat anti-mouse IgG (H+L) (Jackson ImmunoResearch Laboratories Inc., West Grove, PA) used as the capture and detection reagents, respectively. The line represents the average value of the data.)